Biodegradation (2021) 32:87–98
https://doi.org/10.1007/s10532-020-09923-w

ORIGINAL PAPER

Conversion of full nitritation to partial nitritation/anammox in a continuous granular reactor for low-strength ammonium wastewater treatment at 20 °C

Feiyue Qian · Ziheng Huang · Yuxin Liu · Olatidoye Omo wumi Grace · Jianfang Wang · Guangyu Shi

Received: 12 November 2020 / Accepted: 14 December 2020 / Published online: 15 January 2021

Abstract The feasibility of converting full nitritation to partial nitritation/anammox (PN/A) at ambient temperature (20 °C) was investigated in a continuous granular reactor. The process was conducted without anammox bacteria inoculation for the treatment of 70 mg L^{-1} of low-strength ammonium nitrogen wastewater. Following the stepwise increase of the nitrogen loading rate from 0.84 to 1.30 kg N m^{-3} d^{-1} in 320 days of operation, the removal efficiency of total inorganic nitrogen (TIN) exceeded 80% under oxygen-limiting conditions. The mature PN/A granules, which had a compact structure and abundant biomass, exhibited a specific TIN removal rate of 0.11 g N g^{-1} VSS d^{-1} and a settling velocity of 70.2 m h^{-1}. This was comparable with that obtained at above 30 °C in previous reports. High-throughput pyrosequencing results revealed that the co-enrichment of aerobic and anaerobic ammonium-oxidizing bacteria identified as genera *Nitrosomonas* and *Candidatus* Kuenenia, which prompted a hybrid competition for oxygen and nitrite with nitrite-oxidizing bacteria (NOB). However, the overgrowth of novel NOB *Candidatus* Nitrotoga adapted to low temperatures and low nitrite concentration could potentially deteriorate the one-stage PN/A process by exhausting residual bulk ammonium under long-term excessive aeration.

Keywords Nitritation · Anaerobic ammonium oxidation · Granular sludge · Continuous flow reactor · Ambient temperature · Low-strength ammonium wastewater

Introduction

In contrast to the conventional activated sludge system combining nitrificaiton and denitrificaiton, anaerobic ammonium oxidation (anammox) is characterized by carbon source independence, relatively lower oxygen consumption, and low sludge production, among others, allowing efficient nitrogen removal and energy neutral/positive wastewater treatment by separating the removal of nitrogen from the degradation of organic matter (Siegrist et al. 2008; Gao et al. 2014). Partial nitritation/anammox (PN/A) is extensively applied in the treatment of wastewaters with high

Supplementary Information The online version contains supplementary material available at https://doi.org/10.1007/s10532-020-09923-w.

F. Qian (✉) · Z. Huang · Y. Liu · O. O. w. Grace · J. Wang · G. Shi
College of Environmental Science and Engineering, Suzhou University of Science and Technology, No. 1 Kerui Road, Suzhou 215009, People's Republic of China
e-mail: qfywater@163.com

F. Qian · J. Wang · G. Shi
National and Local Joint Engineering Laboratory of Municipal Sewage Resource Utilization Technology, Suzhou 215009, People's Republic of China

nitrogen concentrations (> 100 mg L^{-1}) under mesophilic conditions (> 30 °C) (Huynh et al. 2019). In such conditions, aerobic ammonium-oxidizing bacteria (AOB) oxidize nearly half the amount of ammonium into nitrite, then anammox bacteria (AMX) convert residual ammonium and nitrite into nitrogen gas, thus producing a small amount of nitrate in anoxic niches. The whole process is shown in Eq. (1):

$$\begin{aligned} NH_4^+ + 0.79O_2 + 0.079HCO_3^- \\ \rightarrow 0.010C_5H_7O_2N + 0.028CH_2O_{0.5}N_{0.15} \\ + 0.438N_2 + 0.11NO_3^- + 1.46H_2O + 1.031H^+ \end{aligned} \quad (1)$$

However, PN/A process for completely autotrophic nitrogen removal in low-strength and large-capacity influent, such as municipal wastewater, poses several challenges. These include the effective retention of slow-growing AOB and AMX in continuous-flow mode, the suppression and /or wash-out of nitrite-oxidizing bacteria (NOB) without the inhibition of free ammonia (FA) and free nitrous acid (FNA), and the maintenance of enough activity of AMX communities at ambient temperature (< 25 °C) (Cao et al. 2017).

Compared to early sequencing batch reactors (SBR) applied in PN/A process, the continuous granular reactor is advantageous in large-scale wastewater treatment. By successfully separating the cell and hydraulic retention times, the continuous granular reactor has a nitrogen removal rate ($\sim$ 3.9 kg N m^{-3} d^{-1}) that is significantly higher than the conventional activated sludge (Qian et al. 2018). The high performance of PN/A granules relies on the co-existence of and activity balance between AOB and AMX with adequate biomass, and the prevention of NOB overgrowth. There have been numerous attempts to operate a one-stage PN/A reactor securely at low temperatures through accurate aeration control and effective biomass retention. Such attempts have found that a decrease in temperature from over 20 °C to below 10 °C can result in a marked drop in the total inorganic nitrogen (TIN) removal by more than 50%, along with considerable microbial community shifts driven by cold acclimation (Lotti et al. 2014a; Gonzalez-Martinez et al. 2016; Zhu et al. 2017).

The specific growth rate (μ_{max}) of AMX can reach 0.118–0.334 d^{-1} (doubling time, t_d of 2.2–5.8 days) at 30–37 °C (Liu and Ni 2015; Zhang et al. 2017). The μ_{max} of AMX can significantly decrease to 0.02 d^{-1} (t_d = 35 days) at 20 °C (Lotti et al. 2014b), and to 0.009 d^{-1} (t_d = 79 days) at 12.5 °C (Laureni et al. 2015). This indicates that forming natural PN/A granules with adequate AMX biomass is time consuming at low temperatures. According to Qian et al. (2017), the startup of a PN/A continuous granular reactor without AMX inoculation can be achieved within 5 months at 30 °C, wherein nitritation granules are employed as the seed sludge in influent with ammonium nitrogen (NH_4^+-N) concentration exceeding 100 mg L^{-1}. To the best of our knowledge, a similar shift from full nitritation to PN/A process based on granules at low temperatures and low NH_4^+-N concentration has not been studied adequately. This research gap poses an immense challenge to reactor operations.

Thus, this study aimed to investigate the feasibility of operating PN/A process in a continuous granular reactor without AMX inoculation at an ambient temperature of 20 °C to treat low-strength influent with NH_4^+-N of 70 mg L^{-1}. A stepwise increase in the nitrogen loading rate (NLR) coordinated with aeration intensity was used to drive changes in the sludge morphology and nitrogen-converting performance of the continuous granular reactor. To develop a feasible long-term control strategy of a one-stage PN/A system, experimental evidence of the variations in the bacterial community structure of the granules was obtained using kinetics activity tests and the high-throughput pyrosequencing technique.

Materials and methods

Reactor setup and seed sludge

A continuous stirred tank reactor (CSTR) with a 1.7 L effective volume was used to start up the PN/A process. Liquid was mixed completely by introducing fine bubbles through an air diffuser at the bottom, combined with hydraulic internal recycling, as described in our recent study (Qian et al. 2017).

The seed granular sludge adapted to the removal of organics (as sodium acetate) and ammonia nitrogen was obtained from a lab-scale SBR reactor, which was operated at the influent C/N ratio of 2:1 (Wang et al. 2018). The seed sludge had a milky color and a

compact and round-shaped structure (Fig.S1), a mean size of 0.62 mm, and a sludge volume index after 5 min of sedimentation (SVI_5) of 33 mL g^{-1}. The initial concentration of mixed liquor volatile suspended solid (MLVSS) in the CSTR was set at around 5600 mg L^{-1}.

Reactor operation

Considering the influence of the rejection water and efficient organics degradation in the pretreatment process of integrated wastewater treatment system (Morales et al. 2015), the CSTR was operated with synthetic inorganic media as model low-strength ammonium influent with the following composition (mg L^{-1}): 269.4 NH_4Cl (70.3 ± 2.4 NH_4^+-N), 600 $NaHCO_3$, 8.8 KH_2PO_4/11.2 K_2HPO_4 (as 4 PO_4^{3-}-P basis), 10.0 Na_2EDTA, 5.0 $MgSO_4$, with dosing 1 ml trace element solution (Qian et al. 2018). The pH value was adjusted to 7.8 ± 0.2 with the addition of 10% NaOH solution.

Four operational phases (I-IV) were conducted in 320 days. The volumetric NLR as NH_4^+-N was initially set at 0.84 kg N m^{-3} d^{-1}, which reached 1.30 kg N m^{-3} d^{-1} following a stepwise decrease in the hydraulic retention time (HRT) from 2.0 to 1.3 h (Table 1). During the operation period, the concentration of dissolved oxygen (DO) was controlled in the range of 0.4–1.8 mg L^{-1} by adjusting the air flow rate from 0.5 to 1.2 L min^{-1}. In addition, the temperature was maintained at 20 ± 1 °C using a water bath. Granular biomass was not drained unless sampling for the microbial characterization.

Chemical analysis methods

NH_4^+-N, NO_2^--N, NO_3^--N and MLVSS concentrations, and SVI_5 value were measured using the procedure described in Standard Methods (APHA 1998), and the concentration of TIN was the sum of NH_4^+-N, NO_2^--N and NO_3^--N ones. The DO concentration and pH value were monitored with H1946N portable meters (WTW, Germany). The nitrite accumulation percent (NAP) equaled the mass ratio of NO_2^--N/(NO_2^--N + NO_3^--N) in the effluent, and the ratio of the produced NO_3^--N to the consumed NH_4^+-N was defined as f value. The concentrations of FA and FNA were calculated according to the study of Anthonisen et al. (1976). Where required, Student's t testing was employed to analyze the significance of numerical difference.

The size distribution of the granules was described based on sludge weight percent in four fractions, including < 0.3 mm, 0.3–0.5 mm, 0.5–0.8 mm, and 0.8–1.0 mm. The settling velocity of granules was measured in a vertical glass tube (1000 mm high) filled with water. The formaldehyde-NaOH method was used to extract extracellular polymeric substances (EPS) from the granules, where the quantification of protein (PN) and polysaccharide (PS) was conducted using the Lowry and phenol–sulfuric acid methods, respectively (Pellicer-Nàcher et al. 2013).

Kinetics activity testing

The granule samples were harvested regularly then washed with phosphate buffer solution (pH 7.5) to remove the bulk substrate. Batch activity tests were carried out in a series of 500 mL beakers equipped with an air diffuser for aeration, which contained 400 mL of the synthetic wastewater (identical to the CSTR influent). The inoculate biomass was equally set at 5.0 ± 0.3 g L^{-1} as MLVSS. The batch tests were operated at a DO concentration higher than 3 mg L^{-1}. An approximate complete-mix pattern of granules was maintained at 20 °C. During a 120 min period, a small

Table 1 Description of operating conditions at different phases

Phase	Time (d)	Influent NH_4^+-N concentration (mg L^{-1})	Hydraulic retention time (h)	Nitrogen loading rate (kg N m^{-3} d^{-1})	DO concentration (mg L^{-1})
I	1–69	70.3 ± 2.4	2.0	0.84 ± 0.03	0.4–0.6
II	70–184		1.5	1.13 ± 0.04	0.6–0.8
III	185–264		1.3	1.30 ± 0.04	1.0
IV	265–320		1.3	1.30 ± 0.04	1.8

volume of the supernatant was regularly sampled to analyze the nitrogen compound concentration. Each test was performed in triplicate, and the specific nitrogen conversion rates were calculated using the following equations:

$$q(NH_4^+\text{-N}) = -\Delta c(NH_4^+\text{-N})/(\Delta t \cdot VSS) \quad (2)$$

$$q(NO_2^-\text{-N}) = \Delta c(NO_2^-\text{ N})/(\Delta t \cdot VSS) \quad (3)$$

$$q(NO_3^-\text{-N}) = \Delta c(NO_3^-\text{-N})/(\Delta t \cdot VSS) \quad (4)$$

$$q(TIN) = -\Delta c(TIN)/(\Delta t \cdot VSS) \quad (5)$$

where $q(NH_4^+\text{-N})$, $q(NO_2^-\text{-N})$, $q(NO_3^-\text{-N})$ and $q(TIN)$ are the specific NH_4^+-N removal, NO_2^--N and NO_3^--N accumulation and TIN removal rates, respectively, mg N g^{-1} VSS h^{-1}; $\Delta c(NH_4^+\text{-N})$, $\Delta c(NO_2^-\text{-N})$, $\Delta c(NO_3^-\text{-N})$, and $\Delta c(TIN)$ are the differences in NH_4^+-N, NO_2^--N, NO_3^--N, and TIN concentrations during Δt, respectively, mg L^{-1}; Δt is the reaction time corresponding to the linear variation of nitrogen compound concentration, h; and VSS is the concentration of MLVSS, g L^{-1}.

DNA extraction and high-throughput pyrosequencing

High-throughput pyrosequencing technique was employed to characterize bacterial community structure of the granules as described by Qian et al. (2018). Briefly, four representative sample groups of the granules (G1, G2, G3 and G4) were collected on day 1, 68, 204 and 310 in triplicate respectively, and stored at − 80 °C until genomic DNA was extracted using E.Z.N.A.® Soil DNA Isolation Kit (Omega Bio-tek, Inc., U.S.). The primer pair 338F (5′-ACTCCTACGGGAGGCAGCA-3′) and 806R (5′-GGACTACHVGGGTWTCTAAT-3′) was chosen to amplify the V3-V4 regions of the 16S rRNA gene. The polymerase chain reaction (PCR) mixture composition and amplification program were carried out, and combined PCR products were purified and quantified as recommended. High-throughput pyrosequencing was performed on the Illumina Miseq platform (Illumina, U.S.) at Majorbio Bio-Pharm Technology Co., Ltd., Shanghai, China.

The qualified sequences had an average length of 444.2 bp. Raw sequence data were deposited to the NCBI Sequence Read Archive database (Accession Number: SRR12997732-SRR12997743). Operational taxonomic units (OTUs) were clustered with 97% similarity cutoff using UPARSE embedded in Qiime, and the most abundant sequences in OTUs were assigned to taxonomic classifications. In addition, the alpha diversity analysis including rarefaction curves, species richness estimators of Chao1 and ace, Shannon and Simpson diversity indexes, and abundance-based coverage were performed with mothur software. Heatmap and principal coordinate analysis (PCoA) were conducted on genus level to compare the bacterial communities of the granules at different operation phases.

Results

Reactor operation

Figure 1 shows the variations of nitrogen compound and biomass concentrations in the 320 days operation period of CSTR. For the first 7 days of inoculation, the removal efficiency of NH_4^+-N concentration increased from 35.5% to 98.1%, with the NAP exceeding 80% in the effluent. Because the seed sludge did not acclimatize to the inorganic feeding and operation mode of the CSTR, both partial disintegration of granules (see below) and the loss of biomass (Fig. 1d) were observed in the subsequent three weeks. Therefore, the production of nitrate increased significantly in the CSTR, with the NAP being as low as 51.1% on day 15. To maintain a stable nitritation process, the DO concentration was adjusted to 0.4 mg L^{-1} by decreasing aeration intensity, while a low mass ratio of DO to NH_4^+-N (≤ 0.1) was employed as control strategy of the CSTR at the expense of NH_4^+-N removal (Poot et al. 2016). With the re-growth of biomass as MLVSS concentration, the NH_4^+-N removal and NAP reached 94.9% and 83.6% on day 50, respectively. After that, relatively stronger aeration was introduced into the CSTR, the DO concentration of 0.6 mg L^{-1} did not deteriorate the nitritation performance of granules, and the nitrite accumulation rate was stable at 0.68 ± 0.04 kg N m^{-3} d^{-1}. Notably, the loss of TIN was only $3.3 \pm 2.4\%$ with a wild fluctuation of f value in the range of 0.1–0.5 during phase I.

On day 70, the NLR was increased to 1.13 kg N m^{-3} d^{-1} by shortening the HRT to 1.5 h,

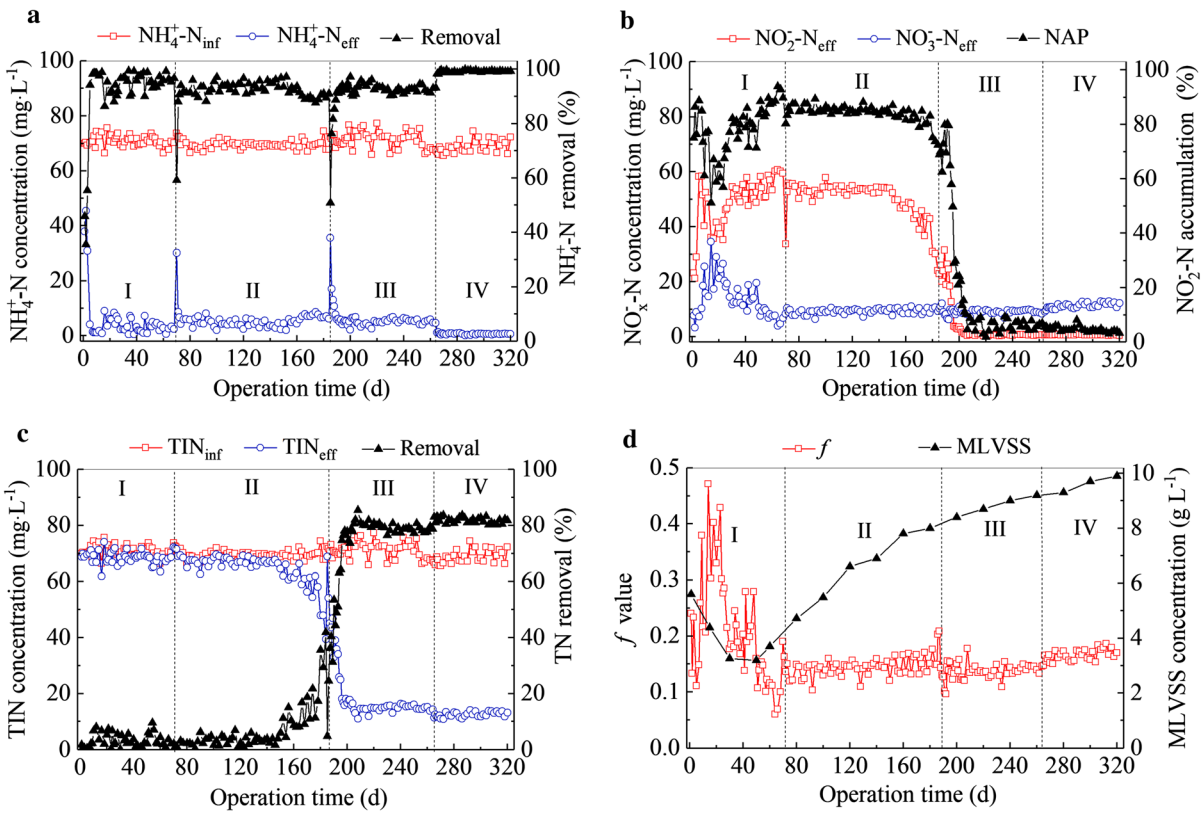

Fig. 1 Variations in **a** NH_4^+-N removal, **b** NO_x^--N production, **c** TIN removal and **d** biomass concentration and *f* value throughout the operation period

with the DO concentration ranging between 0.6 and 0.8 mg L^{-1}. After a short-term impact on the operation of the CSTR, the NH_4^+-N removal rose to 93.9% on day 73. Over the subsequent 80 days, the effluent NO_2^--N of 53.5 ± 1.5 mg L^{-1} was considerably lower than 56.5 ± 3.6 mg L^{-1} at the steady state of phase I (*t* testing, $p = 0.00013$), and the nitrite accumulation rate of 0.85 ± 0.03 kg N m^{-3} d^{-1} was obtained with a negligible TIN loss of 3.2 ± 1.6%. A sudden decrease in the effluent NO_2^--N from 49.7 mg L^{-1} on day 152 to 24.1 mg L^{-1} on day 184 significantly improved the TIN removal. During this period, a stable *f* value of 0.15 ± 0.02 was still higher than the theoretical 0.11 for the PN/A process, and the biomass of granules grew steadily to 8.0 g L^{-1} MLVSS.

In phase III, the CSTR was operated at the NLR of 1.30 kg N m^{-3} d^{-1} and the DO concentration of 1.0 mg L^{-1}, which caused an increase in TIN removal from 24.5% on day 186 to 80.7% on day 205. Compared to the fast startup of the PN/A process in 10–60 days at above 30 °C (Yue et al. 2018; Yang et al. 2019), the conversion of nitritation granules to PN/A types at ambient temperature turned out to be time consuming. However, it was still significantly shorter than 800 days for achieving a TIN removal rate of 0.64 kg N m^{-3} d^{-1} in the anammox process at 20 °C reported by Park et al. (2017). In the successive 60 days of operation, the residual NH_4^+-N in the CSTR was controlled at 5.1 ± 1.0 mg L^{-1}, and the TIN removal of 79.5 ± 1.8% was achieved with a *f* value of 0.14 ± 0.01.

To evaluate the ultimate performance of the CSTR at ambient temperature, the DO concentration was set at 1.8 mg L^{-1} with excessive aeration (phase IV). After day 265, the residual concentration of NH_4^+-N dropped below 1 mg L^{-1}, and the removal efficiency of TIN slightly increased to 81.9 ± 1.0%. Considering the granular biomass of 9.9 g L^{-1} at the end of the operation, the specific TIN removal rate reached approximately 0.11 g N g^{-1} VSS d^{-1}, which was comparable with that obtained by Varas et al. (2015)

at 35 °C under oxygen-limiting condition. However, a noticeable increase in *f* value to 0.17 ± 0.01 (*t* testing, $p \ll 0.00010$) indicated the seeming inevitability of nitrite oxidation to nitrate under ammonium-limiting condition, instead of oxygen limitation.

Granular morphology and kinetics activity

Figure 2 shows the changes in particle size distribution and settling property of the granules over the entire operation period. Granules within the size range of 0.5–0.8 mm were predominant in the seed sludge. The partial disintegration of granules caused a decrease in mean particle size, and the granules that were smaller than 0.3 mm accounted for 47% of the biomass on day 60. Upon the increase in the NLR and improvement in the TIN removal in the CSTR, the mean particle size of granules increased to 0.61 mm on day 320 (Fig. 2a), which was significantly smaller than 1.1–1.9 mm obtained at 30–35 °C (Vlaeminck et al. 2009; Varas et al. 2015). In consistent with the reduction of SVI_5 value, the mature PN/A granules with brownish red (Fig. 2b) exhibited the average settling velocity of 70.2 m h^{-1} with respect to high compactness, which was 2.7 times larger than that of the seed sludge (19.2 m h^{-1}).

EPS play a critical role in cell adhesion, formation of matrix aggregates, improvement of microbial ecology and long-term stability of sludge (Hou et al. 2015). Figure 3 demonstrates that EPS contents in the granules change over time. As the function transformation of granules, the fluctuation of PN contents are clearly more considerable than that of PS contents, and the granules can be characterized by representative PN/PS ratios. At the initial stage of operation, the partial disintegration of granules tended to release loosely-bound EPS contents in the extraction (Wang et al. 2016), corresponding to the PN/PS ratio around 1.36. For the nitritation granules (phase II), a relatively lower EPS contents was determined at the PN/PS ratio of 1.16 ± 0.18. This result is in agreement with those of previous reports, wherein the granules enriched slow-growing nitrifying bacteria had a high proportion of PS in the EPS contents compared with the heterotrophic types (Jemaat et al. 2014; Wang et al.

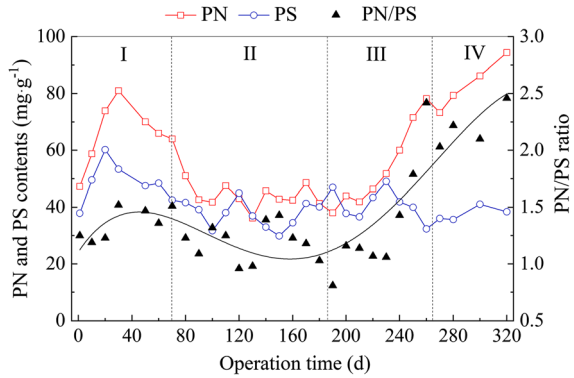

Fig. 3 Variations of EPS contents in granules throughout the operation period

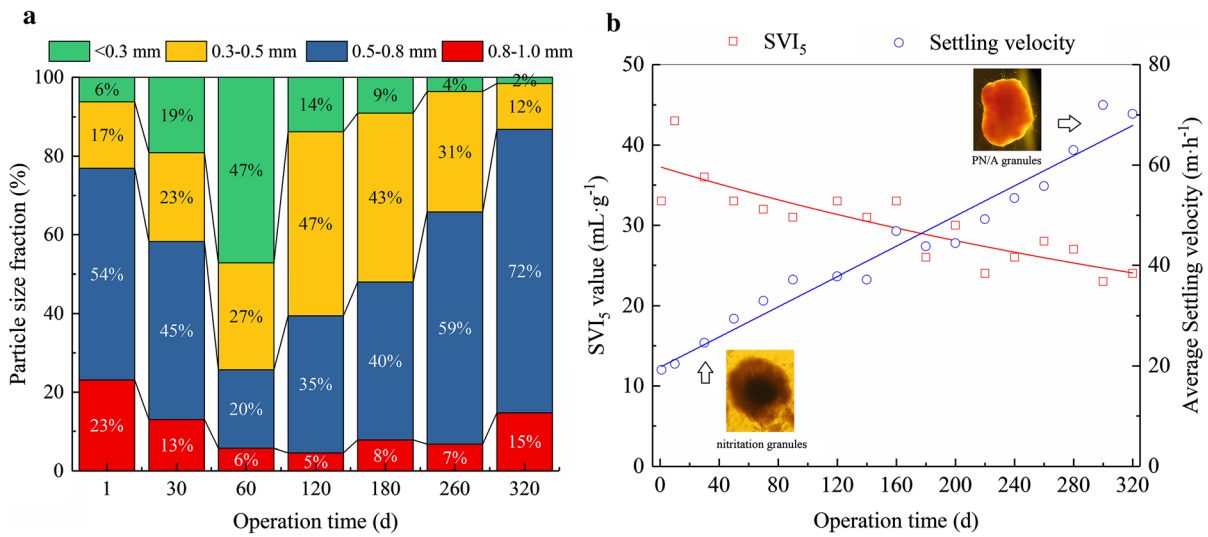

Fig. 2 Changes in **a** particle size distribution and **b** settling property of granules throughout the operation period

2016). Furthermore, a persistent increase in PN was observed following the conversion of granules from full nitritation (phase II) to PN/A process at high NLR (phase IV). The accumulation of EPS contents is crucial in creating substrate gradients in spatial layout of granules, thus allowing for the adherence of AOB in the aerobic shell and protection of AMX in the anoxic core (Vázquez-Padín et al. 2010; Zheng et al. 2016).

As experimental evidence for the kinetics activity of granules, various specific nitrogen conversion rates (q values) were determined using batch tests under high aeration intensity (Fig. 4). Compared with the performance of the CSTR operated under oxygen-limiting conditions, the q values can be considered as good indicators with relatively higher sensitivity for the function transformation of the granules. For the seed sludge, the $q(NH_4^+$-N) was slightly higher than the $q(NO_2^-$-N), while TIN removal and limited production of NO_3^--N were found to be negligible. After day 120, a plateau value of $q(NH_4^+$-N) was obtained with 34.4 ± 1.4 mg N g^{-1} VSS h^{-1}, and the TIN removal was significantly improved following the decrease in $q(NO_2^-$-N) in the subsequent period. This inflection point of time was 30 days in advance to observe a considerable TIN removal in the CSTR. At the end of operation, the ratio of q(TIN) to $q(NH_4^+$-N) for PN/A granules was only 51.1%, and a considerable part of NH_4^+-N was converted to NO_2^--N without further reaction. A credible explanation is that a deeper permeation of DO would be expected with excessive aeration, which significantly inhibited the anammox activity of anoxic core (Vlaeminck et al. 2009). Moreover, the ratio of $q(NO_3^-$-N) to $q(NH_4^+$-N) in batch tests was equal to 0.21, nearly twice as large as the theoretical f value of PN/A process, indicating a high risk of strong nitrite oxidation in the granules (phase IV).

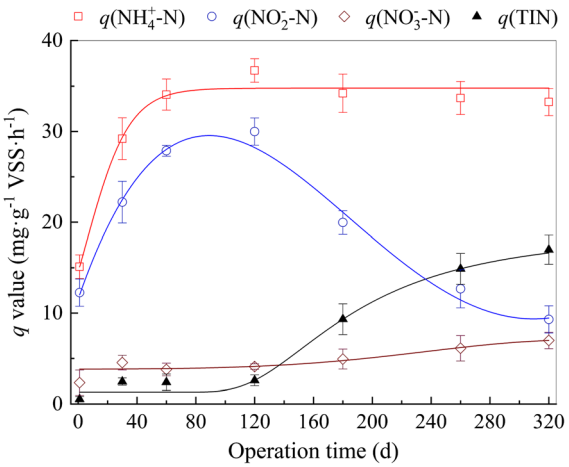

Fig. 4 Variations of specific nitrogen conversion rates of granules throughout the operation period

Microbial community analysis

The microbial community structure of the granules at the different operation phases was analyzed via high-throughput pyrosequencing. A total of 469,411 qualified sequences were obtained and 625 OTUs were identified in the 12 sludge samples belonging to four groups (G1–G4). All the sample coverage estimators exceeded 99.8% with a similar trend of rarefaction curves (Fig. S2). As listed in Table 2, a decrease of the species diversity in G2–G4 was observed, because some heterotrophic bacteria in the seed sludge (G1) would be washed out in the operation of the CSTR with inorganic feeding. Meanwhile, a definite increase in species richness of the granules was associated with efficient sludge retention. As seen in the Venn diagram (Fig. S3), 117 OTUs were shared by the seed sludge (G1) and mature PN/A granules (G4), which accounted for 58.2% and 46.2% of total number in them, respectively.

As shown in Fig. 5, *Proteobacteria* was the most abundant taxon at the phylum level in the granules (mean relative abundance of 59.7–68.2%), followed by *Bacteroidetes*, *Planctomycetes*, and *Chloroflexi.* On the class level, the significant enrichment of *Betaproteobacteria*, *Anaerolineae*, *Planctomycetacia*, and *Nitrospira* was observed during the operation period, with the wash out of *Deltaproteobacteria*, *Sphingobacteriia*, *Gammaproteobacteria*, *Bacilli*, and *Spartobacteria.* Although the granules were fed with inorganic media, satellite heterotrophic bacteria, such as *Sphingobacteriia*, *Anaerolineae*, and *Deltaproteobacteria*, were found and considered to degrade organic macromolecules derived from cells decay and reinforce the EPS matrix (Cho et al. 2011; Chu et al. 2015).

To evaluated the variation of bacterial community structure, PCoA with group dissimilarity was conducted via unweighted UniFrac distance (Deng et al., 2019). As illustrated in Fig. 6a, the seed sludge (G1), nitritation granules (G2), and PN/A granules (G3 and G4) displayed a distinct bacterial community

Table 2 Mean values of recovered sequences, OTU number, and richness/diversity estimators in different sample groups

Group no	Operation time (day)	Read number	OUT number	Richness index		Diversity index		Coverage (%)
				Ace	Chao	Shannon	Simpson	
G1	1	35,135	201	237.75	237.52	3.0592	0.0856	99.8696
G2	79	33,960	240	267.92	274.36	2.8341	0.1707	99.8577
G3	204	40,914	279	333.06	325.80	2.7559	0.2122	99.8267
G4	300	46,461	253	298.01	295.48	2.6465	0.1544	99.8749

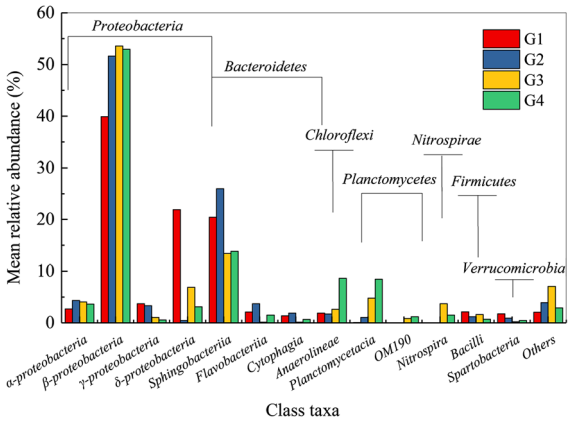

Fig. 5 Bacterial community structures of granules on class taxonomy level

composition on genus level along the first principal coordinate (PCoA1), which accounted for 63.38% of the total variation. Dissimilarity among four sample groups also revealed that the NLR, together with aeration intensity and granular compactness, played an important role in bacterial community shifts (Fig. 6b).

For the seed sludge, genera *Nitrosomonas* (accounted for 12.1%) and *Thauera* (accounted for 19.5%), dominating in the class *Betaproteobacteria*, were identified as the main populations responsible for aerobic ammonium oxidation and nitrite reduction, respectively. NOB and AMX related sequences were not detected (Fig. S4 and S5). Figure 6c shows that an increment of *Nitrosomonas* as AOB fraction was observed in the granules (G2 and G3), while the growth of NOB *Nitrospira* spp. was effectively suppressed under oxygen-limiting conditions. At higher NLR with shorter HRT (phase III and IV), the enrichment of AMX affiliated with genus *Candidatus* Kuenenia (mean relative abundance of 8.4% in G4) was observed and essential for driving the PN/A process, while the AOB/AMX ratio decreased significantly from 9.3 in G3 to 3.6 in G4. This was full consistent with the considerable $q(NO_2^-\text{-N})$ value of mature PN/A granules obtained with excessive aeration in Fig. 4. The co-aggregation cell clusters of *Nitrosomonas* and *Candidatus* Kuenenia in a biofilm PN/A process was also determined with gene expression and biomass concentration measures in conjunction (Park et al. 2015). Although the relative abundance of *Nitrospira* (1.5%) and denitrifiers of *Denitratisoma* (1.1%) in G4 were lower than the ones in G3 (3.7% and 1.8%), respectively, the increase in the f value could not be ignored. It was mainly attributed to the overgrowth of novel NOB identified as genus *Candidatus* Nitrotoga (belonging to class *Betaproteobacteria*) at high DO concentration (phase IV).

Discussion

As mentioned above, nitritaition reaction occurs in the outer portions of the PN/A granules under oxygen-supplied conditions, and the anammox reaction occurs in the inner portions under oxygen-limited conditions. The identification of ecological mechanisms and control strategy for NOB suppression is a prerequisite to the maintenance of the long-term stability of the one-stage PN/A process at ambient temperature.

For most of the operation, the stable suppression of nitrite oxidation to nitrate was obtained under oxygen-limiting conditions in the CSTR, which were achieved by various approaches in different phases. At the beginning of phase I, partial disintegration of the granules brought a low diffusion resistance of oxygen in them, which is favorable for the occurrence of full nitrification at the DO concentration of 0.6 mg L^{-1} (Rathnayake et al. 2015). Thus, the oxygen-limiting condition was maintained at the DO/NH_4^+-N mass

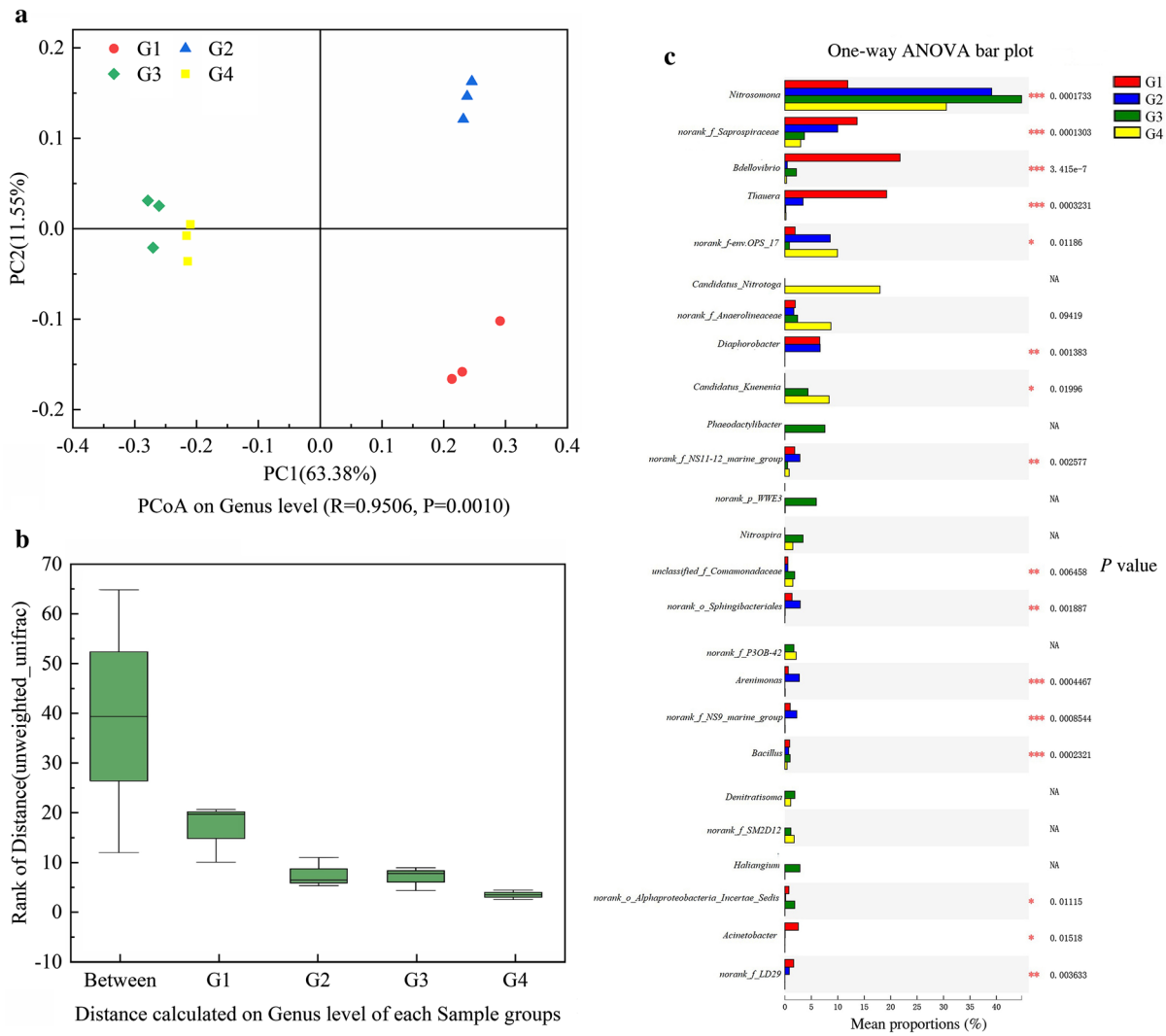

Fig. 6 Bacterial characteristics of granules on genus taxonomy level: **a** principal coordinate analysis (PCoA) plot based on unweighted UniFrac distance from genomic sequencing, **b** rank of distances among four sample groups, and **c** statistical analyses of top 25 genera profiles for pair of sample groups

ratio that was lower than 0.1 for the successful recovery of efficient nitrite accumulation with the NAP over 80% in one month (Fig. 1b). This could be explained by the competitive advantages of AOB abundant in the seed sludge (G1) over common NOB species, because *Nitrosomonas* has higher oxygen affinity (K_O = 0.1–0.3 mg L^{-1}) than *r*-strategist NOB as *Nitrobacter*, and exhibits a larger μ_{max} of 0.77 d^{-1} than 0.25 d^{-1} of *k*-strategist NOB as *Nitrospira* at 20 °C (Cao et al. 2017).

During phase II, higher DO levels did not adversely affect nitritation performance, which was mainly attributable to the improvement of the granular compactness (Fig. 2b) and enrichment of *Nitrosomonas* in granules (G2). This resulted in large diffusion resistance and increased the consumption rate of oxygen in the outer layer of the granules, and favorably inhibited nitrite oxidation to nitrate by NOB (Wang et al. 2016). Unlike the operation of the SBR, the FA (~ 0.1 mg L^{-1}) and FNA (~ 12 μg L^{-1}) levels in the CSTR were too low to suppress NOB and/or AMX in effluent with a pH of 7.6 (Liu et al. 2020).

Notably, a sudden shift from full nitritation to the PN/A process was completed from day 152 to 205

with a significant increase in TIN removal (Fig. 1c). During phase III, the strong aeration accelerated ammonium oxidation in the deeper layer of the granules and promoted mass transfer of nitrite for anammox reaction (Vlaeminck et al. 2009; Xu et al. 2019). Given that the anammox reaction was usually triggered by the accumulation of AMX clusters upon the formation of quorum sensing in the anoxic zone, the slow growth of AMX should begin in the early period (Zhang et al. 2020). As a *k*-strategist with high substrate affinity, *Candidatus* Kuenenia outcompeted the other AMX genera, including Brocadia, Jettenia, Anammoxoglobus and Scalindua, in ammonium-limiting and low temperature environments (De Cocker et al. 2018; He et al. 2018). The increase in AMX abundance offers additional competition for nitrite to suppress NOB in the granules. As a critical control parameter for NOB suppression, sufficient bulk ammonium is responsible for maintaining high activities of AOB and AMX, and stable substrate (DO and NO_2^--N) gradients in the granules, together with EPS accumulation (Lotti et al. 2014a; Pérez et al. 2014). In addition, a settling velocity-based selection pressure was applied in the CSTR with short HRT, which contributed to the wash out of the flocs enriching NOB and the retention of compact granules enriching AMX (Hubaux et al. 2015).

Contrarily, Nitrotoga-like NOB was enriched in the granules (G4) when the ammonium-limiting condition was applied using excessive aeration in phase IV (Fig. 6c). According to previous reports, *Candidatus* Nitrotoga tends to grow at cooling temperatures, and its optimum nitrite concentration is approximately one order and two orders of magnitude below what is usually applied to cultivated *Nitrospira* and *Nitrobacter* (Lebedeva et al. 2008). So far, Nitrotoga-like NOB had been detected using various molecular tools in full-scale wastewater treatment plants operated at 7–16 °C (Lücker et al. 2015), lab-scale continuous anammox reactors operated at 15–17 °C (Liu et al. 2017), and tap water distribution systems under ambient temperature (23–25 °C) (Kinnunen et al. 2017). Lücker et al. (2015) considered that low temperature was one of the main factors supporting high Nitrotoga-like abundances in the activated sludge, and this type of NOB turned out to be active for carbon fixation over a broad range of nitrite concentration (0.1–10 mM) and temperatures (4–27 °C). Because the accumulation of NOB would certainly deteriorate the performance of the PN/A process, further studies concerning the metabolism of Nitrotoga-like NOB and their effects on the granules should be conducted using transcriptomic sequencing. This will lead to the development of a reliable long-term control strategy for continuous reactors at low temperatures.

Conclusions

The conversion of full nitritation to PN/A process at 20 °C was achieved in approximately 200 days of CSTR operation following the stepwise increase of NLR under oxygen-limiting conditions. The mature granules with small particle sizes exhibited a specific TIN removal rate of 0.11 g N g^{-1} VSS d^{-1} and a settling velocity of 70.2 m h^{-1}, comparable with that obtained at above 30 °C in previous reports. This was highly consistent with the co-enrichment of *Nitrosomonas* as AOB and *Candidatus* Kuenenia as AMX in the system. However, the overgrowth of Nitrotoga-like NOB adapted to low temperatures and low nitrite concentration could potentially deteriorate the one-stage PN/A process by exhausting residual bulk ammonium under long-term excessive aeration.

Acknowledgements This study was supported by the National Natural Science Foundation of China (Grant No. 41807142, 51878430), the Open Project of National & Local Joint Engineering Laboratory for Municipal Sewage Resource Utilization Technology (Grant No.2019KF02), and Jiangsu graduate research and practice innovation program, China (Grant No. SJCX20_1101). Authors also acknowledge the support from the Qinglan Project for Jiangsu Colleges and Universities, China.

Compliance with ethical standards

Conflict of interest All authors declare that they have no conflict of interest.

Ethical approval This article does not contain any studies with human participants or animals performed by any of the authors.

References

Anthonisen AC, Loehr RC, Prakasam TBS, Srinath EG (1976) Inhibition of Nitrification by Ammonia and Nitrous Acid. J Water Pollut Control Fed 48:835–852

APHA (1998) Standard methods for examination of water and wastewater, 20th edn. American Public Health Association, New York

Cao Y, van Loosdrecht MC, Daigger GT (2017) Mainstream partial nitritation–anammox in municipal wastewater treatment: status, bottlenecks, and further studies. Appl Microbiol Biotechnol 101:1365–1383

Cho S, Naoki F, Taeho L, Satoshi O (2011) Development of a simultaneous partial nitrification and anaerobic ammonia oxidation process in a single reactor. Bioresour Technol 102:652–659

Chu ZR, Wang K, Li XK, Zhu MT, Yang L, Zhang J (2015) Microbial characterization of aggregates within a one-stage nitritation–anammox system using high-throughput amplicon sequencing. Chem Eng J 262:41–48

De Cocker P, Bessiere Y, Hernandez-Raquet G, Dubos S, Mozo I, Gaval G, Caligaris M, Barillon B, Vlaeminck SE, Sperandio M (2018) Enrichment and adaptation yield high anammox conversion rates under low temperatures. Bioresour Technol 250:505–512

Deng Y, Ruan YJ, Ma B, Timmons MB, Lu HF, Xu XY, Zhao HP, Yin XW (2019) Multi-omics analysis reveals niche and fitness differences in typical denitrification microbial aggregations. Environ Int 132:105085

Gao H, Yaniv DS, George FW (2014) Towards energy neutral wastewater treatment: Methodology and state of the art. Environ Sci: Processes Impacts 16:1223–1246

Gonzalez-Martinez A, Rodriguez-Sanchez A, Muñoz-Palazon G-R (2016) Performance and bacterial community dynamics of a CANON bioreactor acclimated from high to low operational temperatures. Chem Eng J 287:557–567

He S, Chen Y, Qin M, Mao Z, Yuan LM, Niu QG, Tan XC (2018) Effects of temperature on anammox performance and community structure. Bioresour Technol 260:186–195

Hou XL, Liu ST, Zhang ZT (2015) Role of extracellular polymeric substance in determining the high aggregation ability of anammox sludge. Water Res 75:51–62

Hubaux N, Wells G, Morgenroth E (2015) Impact of coexistence of flocs and biofilm on performance of combined nitritation-anammox granular sludge reactors. Water Res 68:127–139

Huynh TV, Nguyen PD, Phan TN, Luong DH, Truong TTV, Huynh KA, Furukawa K (2019) Application of CANON process for nitrogen removal from anaerobically pretreated husbandry wastewater. Int Biodeterior Biodegrad 136:15–23

Jemaat Z, Suárez-Ojeda ME, Pérez J, Carrera J (2014) Partial nitritation and o-cresol removal with aerobic granular biomass in a continuous airlift reactor. Water Res 48:354–362

Kinnunen M, Gülay A, Albrechtsen HJ, Dechesne A, Smets B (2017) Nitrotoga is selected over Nitrospira in newly assembled biofilm communities from a tap water source community at increased nitrite loading. Environ Microbiol 19:2785–2793

Laureni M, Weissbrodt DG, Szivák I, Robin O, Joss A (2015) Activity and growth of anammox biomass on aerobically pre-treated municipal wastewater. Water Res 80:325–336

Lebedeva EV, Alawi M, Maixner F, Jozsa PG, Daims H, Spieck E (2008) Physiological and phylogenetic characterization of a novel lithoautotrophic nitrite-oxidizing bacterium, 'Candidatus Nitrospira bockiana.' Int J Syst Evol Microbiol 58:242–250

Liu LJ, Ji M, Wang F, Yan Z, Tian ZK, Wang SY, Wang SY (2020) Microbial community shift and functional genes in response to nitrogen loading variations in an anammox biofilm reactor. Int Biodeterior Biodegrad 153:105023

Liu WR, Yang DH, Chen WJ, Gu X (2017) High-throughput sequencing-based microbial characterization of size fractionated biomass in an anoxic anammox reactor for low-strength wastewater at low temperatures. Bioresour Techno 231:45–52

Liu YW, Ni BJ (2015) Appropriate Fe (II) Addition Significantly Enhances Anaerobic Ammonium Oxidation (Anammox) Activity through Improving the Bacterial Growth Rate. Sci Rep 5:8204

Lotti T, Kleerebezem R, Hu Z, Kartal B, Jetten MSM, van Loosdrecht MCM (2014a) Simultaneous partial nitritation and anammox at low temperature with granular sludge. Water Res 66:111–121

Lotti T, Kleerebezem R (2014b) Anammox growth on pretreated municipal wastewater. Environ Sci Technol 48:7874–7880

Lücker S, Schwarz J, Gruber-Dorninger C, Spieck E, Wagner M, Daims H (2015) Nitrotoga-like bacteria are previously unrecognized key nitrite oxidizers in full-scale wastewater treatment plants. J - Water Pollut Control Fed 9:708–720

Morales N, Ángeles VR, José RV, Ramón M, Anuska M, José LC (2015) Integration of the Anammox process to the rejection water and main stream lines of WWTPs. Chemosphere 140:99–105

Park H, Sundar S, Ma YW, Chandran K (2015) Differentiation in the microbial ecology and activity of suspended and attached bacteria in a nitritation-anammox process. Biotechnol Bioeng 112:272–279

Park G, Takekawa M, Soda S, Ike M, Furukawa K (2017) Temperature dependence of nitrogen removal activity by anammox bacteria enriched at low temperatures. J Biosci Bioeng 123:505–511

Pellicer-Nàcher C, Domingo-Félez C, Mutlu AG, Smets BF (2013) Critical assessment of extracellular polymeric substances extraction methods from mixed culture biomass. Water Res 47:5564–5574

Pérez J, Lotti T, Kleerebezem R, Picioreanu C, van Loosdrecht MCM (2014) Outcompeting nitrite-oxidizing bacteria in single-stage nitrogen removal in sewage treatment plants: A model-based study. Water Res 66:208–218

Poot V, Hoekstra M, Geleijnse MAA, Van Loosdrecht MCM, Pérez J (2016) Effects of the residual ammonium concentration on NOB repression during partial nitritation with granular sludge. Water Res 106:518–530

Qian FY, Wang JF, Shen YL, Wang Y, Wang SY, Chen X (2017) Achieving high performance completely autotrophic nitrogen removal in a continuous granular sludge reactor. Biochem Eng J 118:97–104

Qian FY, Gebreyesus AT, Wang JF, Shen YL, Liu WR, Xie LL (2018) Single-stage autotrophic nitrogen removal process at high loading rate: granular reactor performance, kinetics, and microbial characterization. Appl Microbiol Biotechnol 102:2379–2389

Rathnayake RMLD, Oshiki M, Ishii S, Segawa T, Satoh H, Okabe S (2015) Effects of dissolved oxygen and pH on

nitrous oxide production rates in autotrophic partial nitrification granules. Bioresour Technol 197:15–22

Siegrist H, Salzgeber D, Eugster J, Joss A (2008) Anammox brings WWTP closer to energy autarky due to increased biogas production and reduced aeration energy for N-removal. Water Sci Technol 57:383–388

Varas R, Guzmán-Fierro V, Giustinianovich E, Behar J, Fernández K, Roeckel M (2015) Startup and oxygen concentration effects in a continuous granular mixed flow autotrophic nitrogen removal reactor. Bioresour Technol 190:345–351

Vázquez-Padín J, Mosquera-Corral A, Campos JL, Méndez R, Revsbech NP (2010) Microbial community distribution and activity dynamics of granular biomass in a CANON reactor. Water Res 44:4359–4370

Vlaeminck SE, Terada A, Smets BF, Clippeleir HD, Willy V (2009) Aggregate Size and Architecture Determine Microbial Activity Balance for One-Stage Partial Nitritation and Anammox. Applied & Environ Microbiol 76:900–909

Wang JF, Qian FY, Liu XP, Liu WR, Wang SY, Shen YL (2016) Cultivation and characteristics of partial nitrification granular sludge in a sequencing batch reactor inoculated with heterotrophic granules. Appl Microbiol Biotechnol 100:9381–9391

Wang JF, Zhang ZY, Qian FY, Shen YL, Qi ZK, Ji XQ, Kajamisso EML (2018) Rapid start-up of a nitritation granular reactor using activated sludge as inoculum at the influent organics/ammonium mass ratio of 2/1. Bioresour Technol 256:170–177

Xu DD, Kang D, Yu T, Ding A, Lin QJ, Zhang M, Hu QY, Zheng P (2019) A secret of high-rate mass transfer in anammox granular sludge: "Lung-like breathing." Water Res 154:189–198

Yang YF, Li Y, Gu ZL, Lu F, Xia SQ, Hermanowicz S (2019) Quick start-up and stable operation of a one-stage deammonification reactor with a low quantity of AOB and ANAMMOX biomass. Sci Total Environ 654:933–941

Yue X, Yu G, Liu Z, Tang J, Liu J (2018) Fast start-up of the CANON process with a SABF and the effects of pH and temperature on nitrogen removal and microbial activity. Bioresour Technol 254:157–165

Zhang L, Narita Y, Gao L, Ali M, Oshiki M, Okabe S (2017) Maximum specific growth rate of anammox bacteria revisited. Water Res 116:296–303

Zhang Q, Fan NS, Fu JJ, Huang BC, Jin RC (2020) Role and application of quorum sensing in anaerobic ammonium oxidation (anammox) process A review. Crit Rev Environ Sci Technol. https://doi.org/10.1080/10643389.2020.1738166

Zheng BY, Zhang L, Guo JH, Zhang SJ, Yang AM, Peng YZ (2016) Suspended sludge and biofilm shaped different anammox communities in two pilot-scale one-stage anammox reactors. Bioresour Technol 211:273–279

Zhu WQ, Li J, Dong HY, Wang D, Zhang PY (2017) Nitrogen Removal performance and operation strategy of anammox process under temperature shock. Biodegradation 28:261–274